Using Demand Response to Improve the Emission Benefits of Wind

Seyed Hossein Madaeni, *Student Member, IEEE* and Ramteen Sioshansi, *Senior Member, IEEE*

Abstract—Although wind generation is emissions- and cost-free, real-time output can be highly variable and uncertain. This can require additional conventional generating capacity to be committed. Since the efficiency of emissions controls can depend on generator loading, this additional capacity can increase generator emissions rates. Another method of accommodating wind is using demand response, which has system loads more closely follow supply. Using a case study based on the Texas power system, we examine the emissions and cost impacts of using these two strategies to accommodate wind. While we find that wind decreases loading and increases emissions rates of generators, it has a positive net emissions benefit overall. We also find that while demand response reduces some of the emissions benefits of wind, combining wind and demand response provides more cost-effective emissions abatement than wind alone.

Index Terms—Wind generation, power system emissions, demand response

Nomenclature

A. Optimization Model Sets and Parameters

T: set of hours in optimization horizon

Ξ: set of scenarios in scenario tree

G: set of conventional generators

Ω: set of wind generators

π_ξ: probability of scenario ξ

$c_g^v(\cdot)$: generator g's variable cost

c_g^n: generator g's spinning cost

c_g^s: generator g's startup cost

K_g^-: generator g's minimum generation level when it is online

K_g^+: generator g's maximum generation level when it is online

R_g^-: maximum amount generator g can rampdown generation in an hour

R_g^+: maximum amount generator g can rampup generation in an hour

$\bar{\rho}_g^{sp}$: maximum amount of spinning reserves generator g can provide in an hour

$\bar{\rho}_g^{ns}$: maximum amount of non-spinning reserves generator g can provide in an hour

τ_g^-: generator g's minimum down-time when shutdown

τ_g^+: generator g's minimum up-time when started up

S. H. Madaeni was with the Integrated Systems Engineering Department, The Ohio State University, Columbus, OH 43210, USA. He is now with the Short Term Electric Supply Department, Pacific Gas and Electric Company, San Francisco, CA 94105, USA (e-mail: SHM8@pge.com).

R. Sioshansi is with the Integrated Systems Engineering Department, The Ohio State University, Columbus, OH 43210, USA (e-mail: sioshansi.1@osu.edu).

The opinions expressed and conclusions reached are solely those of the authors and do not represent the official position of Pacific Gas and Electric Company.

$\bar{w}_{t,\omega,\xi}$: maximum generation available from wind generator ω in hour t under scenario ξ

$p_t(\cdot)$: inverse demand function in period t

η^{sp}: spinning reserve requirement, as a percent of hourly load

η^{ns}: non-spinning reserve requirement, as a percent of hourly load

B. Optimization Model Decision Variables

$q_{g,t,\xi}$: energy produced by generator g in hour t under scenario ξ

$\rho_{g,t,\xi}^{sp}$: spinning reserves provided by generator g in hour t under scenario ξ

$\rho_{g,t,\xi}^{ns}$: non-spinning reserves provided by generator g in hour t under scenario ξ

$u_{g,t}$: binary variable indicating if generator g is online in hour t

$s_{g,t}$: binary variable indicating if generator g is started up in period t

$h_{g,t}$: binary variable indicating if generator g is shutdown in hour t

$w_{t,\omega,\xi}$: energy produced by wind generator ω in hour t under scenario ξ

$l_{t,\xi}$: load served in hour t under scenario ξ

C. Emissions Model Parameters

$\phi_{g,p}(f)$: emissions rate of pollutant p from generator g as a function of the amount of fuel burned, f

N: set of emissions observations in continuous emissions monitors (CEMs) data

$K(\cdot)$: kernel function

$\phi_{g,p}^n$: emissions rate of pollutant p by generator g in observation n in CEMs data

f_g^n: fuel burned by generator g in observation n in CEMs data

h: bandwidth of kernel estimator

D. Cost Model Parameters

W_a: annual social welfare when day-ahead unit commitment decisions are made with wind forecasts with an error variance of a

W_0: annual social welfare when day-ahead unit commitment decisions are made with perfect foresight of wind availability

I. Introduction

RECENT years have seen increased interest in renewable electricity, such as wind and solar, in the United States and elsewhere. This interest is driven by several factors, including concerns surrounding greenhouse gas and other emissions from fossil-fueled generators. Although wind is emission-free, its impact on power system emissions depends on how the variability and uncertainty of real-time wind generation is accommodated. One approach is to use fast-responding conventional generators to balance wind generation. Case studies show that such an approach can increase system operation costs by up to $5/MWh of wind generation [1]–[3].

Wind variability and uncertainty can also be accommodated using demand response (DR). DR allows loads to respond to wind availability, reducing the need for additional generating capacity to be committed and redispatched in real-time. Papavasiliou and Oren [4] study the use of direct load control, wherein deferrable loads are coupled with and dispatched to accommodate wind availability. They develop two solution methodologies for scheduling the loads and use a case study to demonstrate that such a scheme has energy and capacity value in the market. Klobasa [5] examines the effects of DR in a future German power system with 48 GW of wind, showing that DR can reduce wind balancing costs to less than €2/MWh. Sioshansi [6] studies the Texas (ERCOT) system with 14 GW of wind and real-time pricing (RTP). He shows that RTP can eliminate up to 93% of redispatch costs associated with wind, depending on the price-responsiveness of the demand. Dietrich *et al*. [7] use a unit commitment model to examine the impacts of demand shifting and peak shaving on wind integration. They show that these DR programs can have savings of up to 30%, depending on wind availability.

An unexplored question, which is the focus of this paper, is the emissions impact of renewables, when accounting for resource variability and uncertainty and interactions with RTP. In many power systems natural gas-fired generators are used for balancing, due to their ramping capabilities and cost structure. Katzenstein and Apt [8] examine emissions when a natural gas-fired generator is used to balance wind output. They demonstrate that when accounting for generator ramping, emissions can be considerably higher than if the output of the wind plant is constant. This is largely because the heat rate of and the efficiency of emissions controls in a generator can vary depending on whether it is partially loaded. Katzenstein and Apt estimate that wind achieves about 80% of the CO_2 reductions that would be possible without wind variability. They also demonstrate that NO_x emissions are considerably more sensitive. If the generators providing balancing energy use steam-injection NO_x controls, wind achieves about 30–50% of the emissions reductions that would be possible without wind variability. NO_x emissions can increase in net, however, when wind is added if the balancing generators use dry NO_x controls.

In this paper, we extend our previous analysis of wind and RTP [6], which focuses on operational and cost impacts only, to study system emissions. We use the same case study, based on the ERCOT system, to examine how wind and RTP, individually and together, affect generator CO_2, SO_2, and NO_x

emissions. Our analysis shows that if wind is accommodated using dispatchable generators only, the net emissions impacts of wind is considerably more favorable than the work of Katzenstein and Apt suggests. We also demonstrate that using RTP to mitigate the impacts of wind uncertainty and variability increases system emissions relative to having fixed loads. However, RTP also significantly reduces the costs associated with wind variability and uncertainty. When accounting for these two impacts, wind and RTP together deliver much greater emissions reductions per dollar of additional system dispatch costs, compared to having wind only. The remainder of this paper is organized as follows: section II details the unit commitment and dispatch model, emissions and cost calculations, and case study underlying our analysis. We also compare our model, especially simulated emissions in the base case, to historical data. Section III summarizes our results while section IV concludes.

II. MODEL AND CASE STUDY

Our case study is based on the ERCOT power system using 2005 load and conventional generator data. The system had 355 conventional generators in 2005, all of which are modeled. Load and modeled wind availability data from 2005 are used. We assume that the system has 14 GW of wind capacity, which is about 18% of the total installed generating capacity in 2005. This accounts for all of the wind plants that were planned to be built by the end of 2011, and we use wind data corresponding to the locations of these plants.

We model system operations using stochastic day-ahead unit commitment and real-time dispatch models. The unit commitment model determines generator commitments day-ahead, using a scenario tree of wind availability forecasts. The dispatch model determines the real-time output of the committed plants. If a suitable wind availability distribution is used, a stochastic unit commitment can provide operating cost savings relative to a deterministic model [9]–[11]. This is because including multiple wind-availability scenarios can result in more flexible generators, that can more efficiently react to real-time wind availability, being committed.

We also simulate unit commitment and dispatch in a counterfactual case in which wind availability is known with perfect foresight when making commitment decisions day-ahead. Differences in operating costs between cases in which the system is committed using wind forecasts and perfect foresight measure the additional costs imposed on the system by wind uncertainty, which we hereafter refer to as wind-uncertainty costs. We also use the simulated commitments and dispatches in the different cases to estimate generator emissions of CO_2, SO_2, and NO_x.

A. Unit Commitment and Dispatch Model

Our model optimizes unit commitment and dispatch decisions in a rolling fashion 24 hours at a time. We roll through each day of the year, first determining unit commitment decisions (*i.e.* which generators are on- and off-line in each hour) day-ahead when wind availability is not known. This is done using a 48-hour optimization horizon. The additional day

is included in this model to ensure that sufficient generating capacity remains committed in hour 24 to serve the following day's load [6], [12]. A two-stage scenario tree, a schematic of which is shown in Fig. 1, is used to represent uncertain wind output, which is the only stochastic parameter modeled. The scenario tree structure assumes that unit commitment decisions are made in stage 1, when wind output during the 48 hours is unknown. In stage 2, the generation, reserve, and load served decisions are made with full knowledge of wind output over the 48 hours. This scenario tree structure is represented in our model by having the binary generator state variables, $u_{g,t}$, $s_{g,t}$, and $h_{g,t}$, be scenario-independent (*i.e.* there is no ξ subscript), whereas the dispatch variables, $q_{g,t,\xi}$, $\rho_{g,t,\xi}^{sp}$, $\rho_{g,t,\xi}^{ns}$, $w_{t,\omega,\xi}$, and $l_{t,\xi}$ are scenario-dependent. Because the decision variables explicitly embed the structure of the scenario tree, no non-anticipativity constraints are needed in our formulation. The inclusion of multiple wind-availability scenarios in stage 2 is meant to ensure that the generators committed can serve the load under different wind-availability realizations. Our model and scenario tree structure are similar to those used in the works of Ruiz *et al.* [13] and Papavasiliou *et al.* [14].
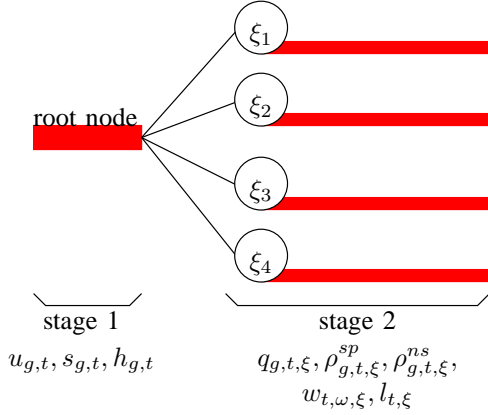
Fig. 1. Scenario tree schematic.

Once these commitment decisions are made, the system is dispatched in real-time based on actual wind output. Generator commitments are fixed in this dispatch problem based on the day-ahead solution, except that we allow fast-start generators that can be started up in less than 15 minutes (*e.g.* natural gas-fired combustion turbines) to be started up if necessary.

1) Stochastic Day-Ahead Unit Commitment Model: The model is given by:

$$
\max \quad \sum_{\xi \in \Xi} \sum_{t \in T} \pi_\xi \cdot \left\{ \int_0^{l_{t,\xi}} p_t(x)dx - \sum_{g \in G} \left[c_g^v(q_{g,t,\xi}) \right. \right. \tag{1}
$$
$$
\left. \left. + c_g^n \cdot u_{g,t} + c_g^s \cdot s_{g,t} \right] \right\};
$$

$$
\text{s.t.} \quad l_{t,\xi} = \sum_{\omega \in \Omega} w_{t,\omega,\xi} + \sum_{g \in G} q_{g,t,\xi}; \quad \forall\, t \in T, \xi \in \Xi; \tag{2}
$$

$$
\sum_{g \in G} \rho_{g,t,\xi}^{sp} \geq \eta^{sp} \cdot l_{t,\xi}; \quad \forall\, t \in T, \xi \in \Xi; \tag{3}
$$

$$
\sum_{g \in G} (\rho_{g,t,\xi}^{sp} + \rho_{g,t,\xi}^{ns}) \geq (\eta^{sp} + \eta^{ns}) \cdot l_{t,\xi}; \tag{4}
$$

$$
\forall\, t \in T, \xi \in \Xi;
$$

$$
K_g^- \cdot u_{g,t} \leq q_{g,t,\xi}; \quad \forall\, g \in G, t \in T, \xi \in \Xi; \tag{5}
$$

$$
q_{g,t,\xi} + \rho_{g,t,\xi}^{sp} \leq K_g^+ \cdot u_{g,t}; \tag{6}
$$

$$
\forall\, g \in G, t \in T, \xi \in \Xi;
$$

$$
q_{g,t,\xi} + \rho_{g,t,\xi}^{sp} + \rho_{g,t,\xi}^{ns} \leq K_g^+; \tag{7}
$$

$$
\forall\, g \in G, t \in T, \xi \in \Xi;
$$

$$
0 \leq \rho_{g,t,\xi}^{sp} \leq \bar{\rho}_g^{sp} \cdot u_{g,t}; \quad \forall\, g \in G, t \in T, \xi \in \Xi; \tag{8}
$$

$$
0 \leq \rho_{g,t,\xi}^{ns} \leq \bar{\rho}_g^{ns}; \quad \forall\, g \in G, t \in T, \xi \in \Xi; \tag{9}
$$

$$
R_g^- \leq q_{g,t,\xi} - q_{g,t-1,\xi}; \quad \forall\, g \in G, t \in T, \xi \in \Xi; \tag{10}
$$

$$
q_{g,t,\xi} - q_{g,t-1,\xi} + \rho_{g,t,\xi}^{sp} + \rho_{g,t,\xi}^{ns} \leq R_g^+; \tag{11}
$$

$$
\forall\, g \in G, t \in T, \xi \in \Xi;
$$

$$
\sum_{y=t-\tau_g^+}^t s_{g,y} \leq u_{g,t}; \quad \forall\, g \in G, t \in T; \tag{12}
$$

$$
\sum_{y=t-\tau_g^-}^t h_{g,y} \leq 1 - u_{g,t}; \quad \forall\, g \in G, t \in T; \tag{13}
$$

$$
s_{g,t} - h_{g,t} = u_{g,t} - u_{g,t-1}; \quad \forall\, g \in G, t \in T; \tag{14}
$$

$$
0 \leq w_{t,\omega,\xi} \leq \bar{w}_{t,\omega,\xi}; \quad t \in T, \omega \in \Omega, \xi \in \Xi; \tag{15}
$$

$$
l_{t,\xi} \geq 0 \quad t \in T, \xi \in \Xi; \tag{16}
$$

$$
u_{g,t}, s_{g,t}, h_{g,t} \in \{0,1\}; \quad \forall\, g \in G, t \in T. \tag{17}
$$

Objective function (1) maximizes social welfare, which is defined as the difference between the integral (up to the amount of load served, $l_{t,\xi}$) of the inverse demand function and total generation cost. In cases without RTP, the load in each hour is fixed. Thus, the integral term in the objective function is fixed, and maximizing social welfare is equivalent to minimizing generation cost. In cases with RTP, the inverse demand function is represented as a non-decreasing step function, implying that the integrals are convex piecewise-linear functions of the $l_{t,\xi}$'s. The variable generation cost functions, $c_g^v(q_{g,t,\xi})$, are represented as convex piecewise-linear functions of the $q_{g,t,\xi}$'s. These assumptions yield an objective function that is linear and convex in the decision variables.

Constraint set (2) are hourly load-balance requirements, which ensure that demand is exactly served in each hour. Constraint sets (3) and (4) impose load-based spinning and non-spinning reserve requirements. Constraint sets (5) through (7) are generation-limit constraints, which ensure that each generator operates between its minimum and maximum generation level. Constraint sets (6) and (7) also force each generator to remain below its maximum generation level if spinning or non-spinning reserves are called. Constraint sets (8) and (9) limit the amount of spinning and non-spinning reserves each generator can provide and only allow generators to provide spinning reserves when online. Constraint sets (10) and (11) impose ramping limits. The ramp-up constraints also restrict spinning and non-spinning reserves so generators can feasibly provide them if called in real-time. Constraint sets (12) and (13) enforce the minimum up- and down-times when generators are started up and shutdown. Constraint set (14) is a state-transition relation, which defines the generator startup and shutdown state variables in terms of changes in the online

state variables. Constraint set (15) restricts wind generation to be below the maximum amount available. Constraint set (16) forces the load served to be non-negative and constraint set (17) imposes integrality restrictions on the binary state variables.

Our model treats demand response in the cases with RTP as a dispatchable resource that the system operator can use to serve the load. This implicitly assumes that consumers truthfully reveal their willingness to pay for energy and that they adjust their demand in real-time based on the socially optimal dispatch of demand response determined by the system operator. Thus our modeling approach does not tackle the issue of generating market-clearing prices that ensure that suppliers and consumers have proper incentives to provide the socially optimal amount of generation and demand response. This is a theoretically difficult task, due to the non-convex nature of power system operations and unit commitment [15]. Moreover, we assume that consumers can react to real-time signals from the system operator immediately, without any latency. Any delay in the consumer response likely reduces the wind-related benefits of RTP, since the principal benefit of RTP is to have demand more closely follow real-time wind availability.

2) Dispatch Model: The dispatch model is identical to the unit commitment model, except that the commitments (*i.e.* the values of $u_{g,t}$, $s_{g,t}$, and $h_{g,t}$) of all generators that are not fast-start are fixed based on the solution of the day-ahead model. Moreover, the scenario tree is not used and the system is dispatched against actual wind availability. All of the spinning and non-spinning reserve requirements must also be maintained in real-time, and cannot be used to serve wind shortfalls. This is because these contingency reserves are assumed to be used to accommodate unanticipated load increases or conventional generator or transmission failures. The flexible generators committed day-ahead due to the scenario tree are intended to accommodate wind variability. Ruiz *et al.* [13] discuss the advantages and disadvantages of relying on generators committed using a stochastic model, as opposed to using operating reserves, to accommodate wind and other system uncertainties.

3) Model Data: Generator constraint and cost data are obtained from Global Energy Decisions (GED) and Platts Energy. Hourly system load data are obtained from the Public Utility Commission of Texas (PUCT). In cases without RTP, the hourly loads are fixed equal to these historic values. Cases with RTP are modeled by assuming the price elasticity of demand and calibrating the inverse demand function in each hour so the actual historical load in the hour corresponds to the historical average retail price of electricity [6], [12], [16], [17]. Thus, the hour-t demand function is calibrated so:

$$p_t(l_t) = p^{ret}, \qquad (18)$$

where l_t is the historical load in hour t and p^{ret} is the historical retail price of electricity. In doing so we only model own-price elasticities, assuming that cross-price elasticities are zero. This assumption potentially understates the extent to which RTP shifts loads from on- to off-peak hours. This load shifting effect is somewhat captured through modeling only

own-price elasticities, however, since on-peak loads drop (due to relatively high real-time prices) while off-peak loads rise (due to lower prices) [12]. We consider cases with elasticities of -0.1 and -0.3, which are consistent with empirical estimates [18]. Retail electricity price data are obtained from the United States Department of Energy's Energy Information Administration (EIA) and PUCT filings are used to remove non-energy-related costs from the retail price. Each hourly inverse demand function is approximated as a step function with 100 segments. We assume that total reserves, half of which must be spinning reserves, must amount to at least 9% of the hourly load.

We use historical mesoscale model data available in the National Renewable Energy Laboratory's Western Wind Resources Dataset to represent actual hourly wind availability.[1] These data specify what fraction of the installed nameplate capacity of each wind generator is available in each hour. The scenario tree is constructed by adding 'forecast error' terms to the actual wind availability fraction in each hour. Following the assumption used in the California ISO's renewable integration study, we assume that the forecast errors have an unbiased first-order autocorrelated truncated Gaussian distribution [6], [19]. We assume an autocorrelation coefficient of 0.6 and consider cases in which the forecast error has a variance of between 0.0025 and 0.0225 (or error standard deviations between 5% and 15%). A higher variance implies less accurate wind forecasts. We use a scenario tree with four terminal leaves, as shown in Fig. 1. The scenarios are constructed by generating 1000 sample paths of the forecast error terms using Monte Carlo simulation. These 1000 sample paths are reduced to the four leaves constituting the scenario tree, with corresponding probabilities, using the forward selection algorithm in the SCENRED scenario reduction tool available in GAMS [20].

4) Model Implementation: The day-ahead and real-time models are formulated using GAMS and solved using the branch and cut algorithm in CPLEX with default settings. The models are solved using a 64-bit 2.7 GHz Pentium Core 2 processor with 6 GB of RAM. Each day-ahead unit commitment problem has about 280,000 variables and 570,000 constraints and takes an average of 500 s of CPU time to solve.

B. Emissions Modeling

Our analysis only considers emissions directly attributable to the combustion of fuels by generators. Emissions are estimated using input-based emission rates, which specify the mass of each species emitted per unit of fuel burned. We prefer input- to output-based rates, which specify emissions per unit of electricity generated, since they better account for generator startups and the effect of partial loading on generator heat rates. We combine the optimized commitment and dispatch of the generator fleet with heat rates and estimates of generator startup and spinning fuel use to determine hourly fuel consumption by each generator.

---

[1] These data are publicly available for download from the National Renewable Energy Laboratory at http://wind.nrel.gov/Web_nrel/.

Although generator emissions are often estimated using a constant emissions rate [21], this approach does not capture the effect of part-load operation on the efficiency of emission controls. Because wind and RTP can result in load shifting and partially loading generators (*e.g.* to provide capacity to accommodate real-time wind variability), generator emissions rates can change beyond the impacts of heat rate variation. As an example, Fig. 2 shows actual NO_x emissions rates for a combined-cycle natural gas-fired unit as a function of generator loading. These emissions rates are taken from 2005 continuous emissions monitors (CEMs) data reported by the United States Environmental Protection Agency.[2] The figure shows higher than average emissions rates when the generator is partially loaded, which is indicative of the fact that some SO_2 and NO_x emissions controls are relatively inefficient when operated in such a manner. The efficiency of these controls is also sensitive to the technology used (*e.g.* steam-injection versus dry NO_x controls), thus the emissions rates vary between the units modeled.
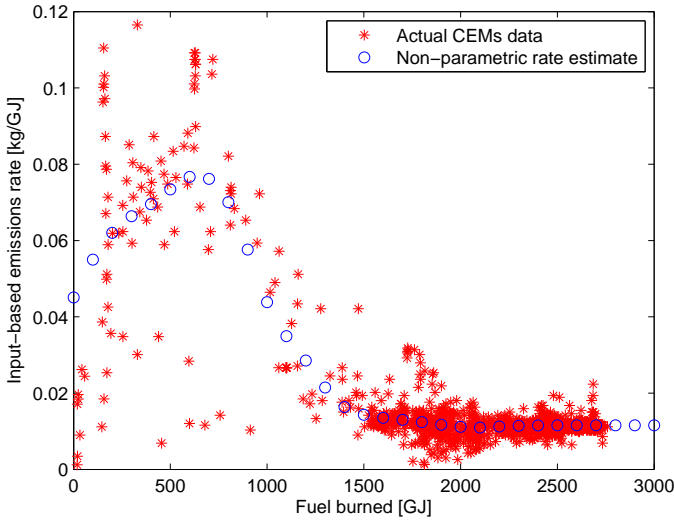
Fig. 2. Actual NO_x emissions rates and non-parametric rate for AES Wolf Hollow 1a combined-cycle natural gas-fired unit during the ozone season.

To capture these effects, we use a non-parametric Nadaraya-Watson kernel estimator of SO_2 and NO_x emissions rates [22]–[24]. This technique estimates a function, $\phi_{g,p}(f)$, which specifies generator g's input-based emissions rate of pollutant p as a function of the amount of fuel burned, f. This function is estimated as:

$$\phi_{g,p}(f) = \frac{\sum_{n \in N} K\left(\frac{f - f_g^n}{h}\right) \phi_{g,p}^n}{\sum_{n \in N} K\left(\frac{f - f_g^n}{h}\right)}. \tag{19}$$

The terms $\phi_{g,p}^n$ and f_g^n in (19) represent the actual emissions rate and amount of fuel consumed, as reported in the CEMs data. The function $K(\cdot)$ is the kernel or smoothing function, and we use the standard Gaussian density function. The bandwidth, h, controls the weight put on neighboring

observations in estimating $\phi_{g,p}(f)$. We use an optimal bandwidth, $h = \mathcal{O}\left(|N|^{-1/4}\right)$, which ensures that the estimator is asymptotically consistent. Fig. 2 shows the non-parametric emissions rate estimate derived using this technique.

We estimate separate SO_2 and NO_x emissions rates functions for each generator that appears in the CEMs data. Because CO_2 emissions are not controlled, fixed input-based emissions rates are estimated from the CEMs data. Since NO_x is an ozone precursor, we differentiate NO_x emissions rates between an ozone (May to September) and a non-ozone (the remaining months) season. This is done by estimating different $\phi_{g,p}(f)$ functions for each generator using CEMs data from the ozone and non-ozone seasons separately. This helps to capture any seasonal difference in the use of NO_x controls, for instance due to more stringent regulations during the ozone season. We use fixed CO_2, SO_2, and NO_x emissions rates, reported by GED, for generators that do not appear in the CEMs data.

C. Wind-Uncertainty Cost

A standard measure of wind-uncertainty cost is the difference between the cost of operating the system when imperfect wind forecasts are used and a counterfactual case in which wind availability is known with perfect foresight [1]–[3]. Because we examine RTP, which allows loads to adjust, the difference in social surplus (as defined by objective function (1) of our MIP) is a more appropriate metric [6]. This is because loads adjustments give consumer surplus changes that are not captured by differences in generation costs. Using this approach, the wind-uncertainty cost when forecasts with an error variance of a are used is given by:

$$W_0 - W_a. \tag{20}$$

This measures the cost of wind uncertainty as the decrease in social welfare caused by using imperfect forecasts when making commitment decisions day-ahead. The perfect foresight cases are simulated using the same day-ahead unit commitment model, but without the two-stage scenario tree. Rather, the commitment and dispatch are optimized assuming that wind availability is perfectly known. Moreover, these cases do not require the dispatch model to be solved, since the day-ahead unit commitment model is solved using the actual wind availability.

D. Model Validation

In order to validate our model, especially the emissions calculations, we compare aggregate system generation and emissions to historical data reported by the EIA. We prefer EIA data to the CEMs, since the latter does not include generators smaller than 50 MW. The EIA reports historical aggregate annual generation, fuel consumption, and emissions in each state. Although the ERCOT region is wholly contained within the state of Texas, some regions of the state are in the western and eastern interconnects. Since ERCOT accounts for roughly 85% of the load of the state of Texas, we scale the EIA data by a factor of 0.85 to estimate the corresponding historical data for ERCOT.

Table I compares modeled generation, fuel consumption, and emissions in the base case in which no additional wind is added to the system and loads are fixed. It also reports the scaled EIA data. Comparing the modeled and EIA data shows that the scaling is roughly correct in capturing total ERCOT loads, since total modeled and EIA-reported generation differ by less than 1%. There is, however, a difference in the breakdown of this generation, with our model resulting in 51% of the load being served by coal-fired generation as opposed to 47% in the EIA data. The modeled and EIA data also reveal differences in the efficiencies of the natural gas-fired generators used. Whereas the modeled natural gas-fired generators have an average heat rate of about 9.9 GJ/MWh, the EIA data gives an average heat rate of about 12.7 GJ/MWh. These heat rate and generation differences could be due to the breakdown of the generator fleet within ERCOT, as compared to the rest of the state. If more low-efficiency natural gas-fired generators tend to be outside of the ERCOT region or more coal-fired generators are within ERCOT, that could result in the emissions differences shown. These differences could also be indicative of the generator fleet outside ERCOT being of an older vintage. Otherwise, it is possible that our model does not include detailed transmission and operating constraints (*e.g.* reliability must-run requirements). These types of constraints can affect which generators are operated in real-time, yielding a different mix of fuels and generator efficiencies.

TABLE I
MODELED BASE CASE AND EIA-REPORTED ANNUAL GENERATION AND EMISSIONS

	Modeled	EIA-Reported
Generation [TWh]		
Total	262.93	263.14
Coal	134.77	123.93
Natural Gas	122.82	139.21
Fuel Consumption [PJ]		
Total	2,727	3,191
Coal	1,510	1,424
Natural Gas	1,217	1,767
CO_2 [Mt]		
Total	198.53	220.27
Coal	136.72	131.31
Natural Gas	61.81	88.96
SO_2 [kt]		
Total	451.16	457.11
Coal	450.75	456.57
Natural Gas	0.41	0.55
NO_x [kt]		
Total	140.37	195.30
Coal	102.05	107.13
Natural Gas	38.32	88.17

These differences in the efficiencies of the natural gas-fired plants largely contribute to the differences in the modeled and EIA-reported emissions. Emissions from the coal-fired plants are largely consistent between the two data sets, with total CO_2, SO_2, and NO_x emissions differing by 6%, 1%, and 5%, respectively. Natural gas-fired generator emissions of CO_2 and NO_x are considerably higher in the EIA-reported data, however, reflecting the higher heat rate.

To further verify this, Fig. 3 shows modeled hourly input-based SO_2 and NO_x emissions rates for the entire natural gas-fired generator fleet as a function of fuel consumption. It also shows hourly input-based emissions rates computed from the CEMs data. While there are differences in the modeled and CEMs-reported emissions rates, they are within a similar range. Some differences in the emissions rates are to be expected, since ramping constraints and commitment decisions affect what specific mix of generators is producing energy and emitting SO_2 and NO_x during any given hour. Since the modeled and CEMs-reported emission rates are similar, the emissions differences are due to the heat rates.
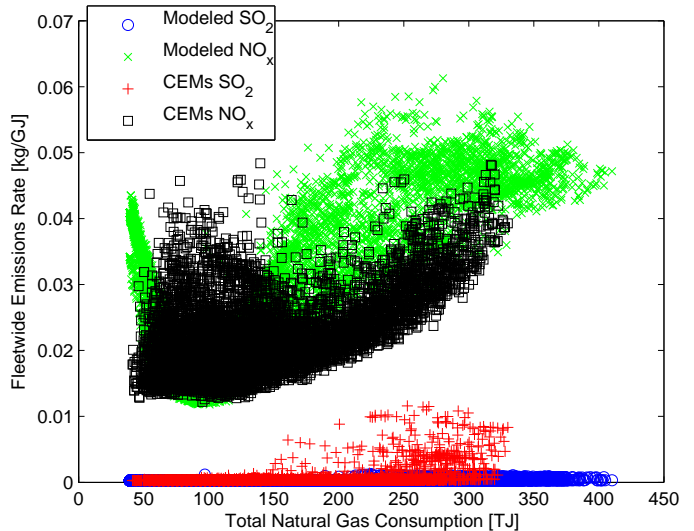
Fig. 3. Modeled and CEMs-reported hourly average input-based emissions rates of SO_2 and NO_x of natural gas-fired generators.

III. RESULTS

A. Emissions Effects of Wind

Table II summarizes the effect of wind on annual generation and emissions without RTP. The added wind displaces roughly 43 TWh of conventional generation, about 27% of which is coal-fired. This yields CO_2 reductions of about 13% and reduces SO_2 and NO_x emissions by 11–12% relative to the no-wind case, depending on wind forecast accuracy. This translates into an average of about 2000 t of CO_2, 3.6 t of SO_2, and 1.2 t of NO_x being eliminated annually per MW of added wind. Table II further shows that emissions decrease as the wind forecasts become less accurate. Less accurate forecasts force more natural gas-fired generators, which have greater ramping capabilities than coal-fired generators, to be committed in order to provide sufficient flexibility to accommodate wind variability. These natural gas-fired plants displace coal-fired generators, giving the emissions savings. This results, however, in natural gas-fired generators increasingly being operated at part load, causing an increase in their emissions rates. This is demonstrated in Table III, which shows the average loading of natural gas-fired generators when they are online and their output-based emissions rates in the fixed-load case. A generator's loading in an hour is defined as the amount of fuel burned in that hour divided by the amount it would

burn if operated at maximum load.[3] Tables II and III show that as the wind forecasts become less accurate, more natural gas-fired generators are committed and operated at a lower average level in order to provide ramping capacity, increasing their emissions rates.

Katzenstein and Apt [8] observe this effect and estimate that cycling and partially loading natural gas-fired plants can result in net NO_x increases when wind is introduced to a system. Contrasting their findings with ours illustrates two issues with their emissions estimation technique, which Mills *et al.* [25] note. One is that they assume that each wind generator must have a dedicated conventional generator that follows its output (*i.e.* each wind plant requires 100% reserves). This eliminates the benefits of a (spatially) diversified wind generator portfolio. Wind diversification can reduce the need for conventional generation to follow the output of individual wind generators, since the output of individual wind plants tend to be less correlated with one another. This reduces the variability of the aggregate wind generation profile. The hourly real-time wind availability of the individual wind plants that we model have coefficients of variation[4] ranging between 0.80 and 1.25. The coefficient of variation of hourly aggregate wind availability across the ERCOT system is 0.76, however. This shows that diversification of wind reduces the variability of aggregate wind output and the need for reserve capacity below the 100% that Katzenstein and Apt assume. Indeed, there is a broad literature focused on estimating reserve requirements with high wind penetrations [26]–[28], and our stochastic unit commitment is intended to ensure that sufficient fast-ramping capacity is available to accommodate wind variability. A second limitation is that Katzenstein and Apt do not account for the effect of wind uncertainty on unit commitment decisions. As illustrated in Table II, inaccurate wind forecasts result in the commitment and generation mix shifting toward natural gas-fired plants. Although these natural gas-fired plants are less loaded, resulting in higher emissions rates, the fuel switching benefits more than outweighs this emissions increase.

B. Emission Effects of Wind and RTP

Because real-time prices and electricity demand are correlated, RTP affects load profiles by reducing on-peak and increasing off-peak demands. This effect is more pronounced if cross-price elasticities are modeled, since on-peak demands decrease both due to the high on-peak price and the relatively low price during shoulder and off-peak hours, to which demand can be shifted. Many power systems, including ERCOT, use a mix of generating fuels (*e.g.* natural gas and coal), thus this change in the load pattern can result in dramatic changes in the generation mix used and resulting system emissions.

Table IV summarizes the effects of wind and RTP on annual emissions, showing that the effect of RTP depends on the presence of wind. In the no-wind case, RTP causes the

[3]Generator loading can also be defined in terms of output. We opt to define it in terms of fuel burned, since this metric also captures fuel use associated with generator startups. Nevertheless, these two definitions are closely related since higher generation requires more fuel.

[4]The coefficient of variation is defined as the ratio between the standard deviation and mean of hourly wind availability.

change in diurnal load patterns discussed above but also yields a reduction in total electricity demand. This is because the retail price of electricity in 2005 was lower than the average real-time price. Thus, exposing consumers to real-time prices results in a greater demand reduction during on-peak periods than the demand increase during off-peak periods. As such, introducing RTP without wind yields a net reduction in all emissions except for SO_2. SO_2 emissions increase because the change in the diurnal load pattern results in the share of coal-fired generation increasing from about 52% of the load without RTP to 53–54% with RTP (depending on the demand elasticity). The significantly higher sulfur content of coal (natural gas- and coal-fired generators in ERCOT release, on average, about 0.0003 and 0.2984 kg of SO_2, respectively, per GJ of fuel burned) yields net SO_2 emissions despite less energy being generated.

This effect of RTP is something of an artifact of the data—if retail and real-time prices are closer to each other, RTP would likely cause a net increase in all emissions. This is because overall demand would see a smaller change but be shifted toward off-peak hours, during which coal-fired generation is marginal. This exact effect is observed in an analysis of the emissions impact of RTP in the PJM system [29]. The low retail prices in 2005 are indicative of the fact that they are set through regulatory mechanisms and can lag the cost of generation by several years. Indeed, EIA data show that the average price of natural gas for the United States's electricity generation sector rose by 39% between 2004 and 2005, which is likely not captured in the 2005 retail electricity rates. We can partially control for this effect by comparing average output-based emissions rates. Table V compares average emissions rates across the entire conventional generator fleet in the fixed-load and RTP cases. The RTP case assumes a demand elasticity of -0.1—the results are similar but greater in magnitude with the higher elasticity. The table shows that if RTP is introduced output-based emissions rates increase relative to the fixed-load case.

When the 14 GW of wind is added to the system, RTP has the effect of increasing system emissions. This is because the added wind suppresses real-time electricity prices and they are, on average, lower than the retail price in 2005. Thus, RTP increases total electricity demand. Moreover, RTP has the same effect of decreasing on-peak and increasing off-peak demand. Thus, the demand shifts toward hours during which coal-fired generation is marginal. Introducing RTP when wind is in the system increases the use of coal-fired generation from 57% of the conventional generation mix to 60%.

C. Cost of Emissions Reductions

Although RTP reduces the emissions benefits of wind, it also significantly reduces wind-uncertainty costs [6]. This synergy between wind and RTP is demonstrated in Fig. 4, which shows hourly actual wind and wind forecasts, as well as system loads on 18 July. Actual wind availability on this day varies from 146 MW to 2.6 GW. Moreover, the accuracy of the wind forecasts vary significantly throughout the day. The wind scenarios modeled between hours 3 and 14 both

TABLE II
ANNUAL GENERATION BREAKDOWN AND GENERATOR EMISSIONS WITH FIXED LOADS

Wind Forecast Error Variance	Generation [TWh]		Total Emissions		
	Coal	Natural Gas	CO_2 [Mt]	SO_2 [kt]	NO_x [kt]
No Wind	134.8	122.8	198.5	451.2	140.4
0.0025	122.9	91.0	172.1	400.7	124.2
0.0100	122.7	91.1	171.9	399.7	124.0
0.0225	122.5	91.4	171.8	398.8	123.8

TABLE III
AVERAGE LOADING AND OUTPUT-BASED EMISSIONS RATES OF NATURAL GAS-FIRED GENERATORS WITH FIXED LOADS

Wind Forecast Error Variance	Average Natural Gas Generator Loading [%]	Natural Gas Emissions Rates		
		CO_2 [kg/MWh]	SO_2 [g/MWh]	NO_x [g/MWh]
0.0025	34.1	523.8	3.59	349.5
0.0100	30.2	523.7	3.59	350.3
0.0225	28.1	523.6	3.61	350.6

TABLE IV
ANNUAL GENERATOR EMISSIONS WITH RTP

Wind Forecast Error Variance	Demand Elasticity -0.1			Demand Elasticity -0.3		
	CO_2 [Mt]	SO_2 [kt]	NO_x [kt]	CO_2 [Mt]	SO_2 [kt]	NO_x [kt]
No Wind	197.0	452.4	138.7	194.3	453.1	135.5
0.0025	173.7	412.7	124.8	176.0	430.1	125.1
0.0100	173.5	412.0	124.7	175.8	429.7	125.0
0.0225	173.3	411.3	124.5	175.7	429.3	124.9

TABLE V
AVERAGE OUTPUT-BASED EMISSIONS RATES OF ALL GENERATORS WITH FIXED LOADS AND RTP

Wind Forecast Error Variance	Fixed Loads			RTP (Demand Elasticity -0.1)		
	CO_2 [kg/MWh]	SO_2 [g/MWh]	NO_x [g/MWh]	CO_2 [kg/MWh]	SO_2 [g/MWh]	NO_x [g/MWh]
No Wind	770.7	1751.4	544.9	773.1	1775.4	544.3
0.0025	803.2	1870.5	579.6	808.7	1921.5	581.0
0.0100	802.5	1866.1	579.0	808.5	1919.9	581.1
0.0225	802.1	1861.9	578.1	808.2	1918.1	580.6

over- and under-estimate wind availability. From hour 15 to 22, however, all of the wind scenarios overestimate wind, with hour 22 having extreme overestimates of between 1.2 and 2.8 GW. This results in less generating capacity being available in the afternoon and the system must commit fast-starting natural gas-fired plants in real-time to serve the load in the fixed-demand case. The lower panel of Fig. 4 demonstrates the benefit of RTP, which is that loads respond to wind availability through price signals. Between hours 15 and 22, for instance, an average of about 600 MW of load is curtailed, reducing the cost of accommodating the unexpectedly low wind generation.

Thus, determining the benefits and synergies between wind and RTP should account for both these cost and emissions effects. Table VI summarizes the annual wind-uncertainty cost, as given by (20), divided by total wind generation. The table shows that less accurate day-ahead wind forecasts increases wind-uncertainty costs. It also shows that increasing demand

responsiveness decreases these costs. This is because demand is better able to respond to unforeseen increases or decreases in wind availability.

TABLE VI
WIND-UNCERTAINTY COST [$/MWH OF WIND]

Wind Forecast Error Variance	Demand Elasticity		
	-0.0	-0.1	-0.3
0.0025	1.81	0.25	0.02
0.0100	3.79	0.99	0.02
0.0225	6.11	1.89	0.04

Table VII summarizes the amount of emissions reductions that wind provides per dollar of wind-uncertainty cost incurred. This is defined as the reduction in generator emissions summarized in Tables II and IV, divided by the wind-uncertainty cost given by (20). Values for the cases with RTP
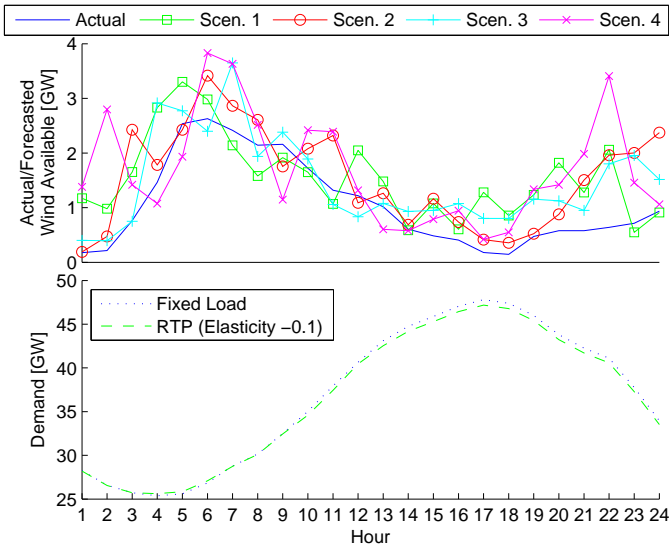
Fig. 4. Actual wind, wind forecasts, and electricity demand on 18 July. Wind forecasts have 0.01 error variances and demand elasticity is −0.1 in the RTP case.

are given as ranges covering the different elasticity values that we consider—the lower-end of the range corresponds to an elasticity of −0.1 and the upper-end to an elasticity of −0.3. These values capture the two effects of RTP and wind together—increased emissions and reduced wind-uncertainty costs. The table demonstrates that although RTP reduces the emissions benefits of wind, the significantly lower wind-uncertainty cost borne by the system more than compensates for this. In some cases, RTP gives emissions savings that are more than two orders of magnitude greater than with fixed loads, showing that RTP is an effective means of integrating wind, when considering both the cost and emissions impacts together.

IV. Conclusion

Our analysis demonstrates that RTP is a cost-effective means of integrating wind into power systems. Although RTP reduces the emissions benefits of wind, the associated cost savings more than compensates for these losses and reduces the wind-uncertainty cost incurred per kg of emissions averted by wind. While less accurate wind forecasts provide incremental emissions benefits by tilting the mix of generators used away from coal, the associated cost increase overwhelms these benefits, as shown in Table VII. Whereas a dollar of wind-uncertainty cost averts up to 3 t of CO_2 with fixed loads, the same dollar can avert up to between 23 and 232 t with RTP.

The combination of wind and RTP can also provide something of a virtuous investment cycle, since lower wind-uncertainty costs can reduce perceived barriers or limits (both technical and financial) to the entry of wind in power systems. Although wind-uncertainty costs are not currently passed onto wind generators (in most markets in the United States), they nevertheless represent real costs borne by power system operators, utilities, and (ultimately) ratepayers. Our analysis focuses on wind and a topic for further investigation is whether RTP and other variable renewables, such as solar, would have

similar synergies. While solar presents the same type of integration challenges, solar generation patterns can be markedly different from wind. Indeed, solar generation peaks midday when prices can peak. Thus, solar and RTP may result in more midday consumption, compared to a fixed-load case, and less shifting of loads to off-peak periods (compared to having wind and RTP together). This can yield very different effects on generation and emissions. Although our analysis focuses on RTP other forms of DR may provide similar benefits, so long as they are sufficiently dynamic to react to real-time wind availability. While our results are based on the ERCOT system, the general findings that RTP can improve the overall cost-effectiveness of wind in reducing generation emissions should be broadly applicable in other power systems. This is because RTP provides system operators with an additional tool to mitigate wind uncertainty and variability. This should result in a cost reduction that outweighs any emissions increases caused by changes in the diurnal load profile.

Our analysis relies on a relatively small scenario tree in the stochastic unit commitment. A larger scenario tree may reduce wind-uncertainty costs. This is because it may better represent the possible range of wind availabilities, resulting in a more appropriate generation mix being committed. We also assume that the system operates in a relatively static manner, with each day's commitment fixed based on the day-ahead forecasts. A more dynamic model, which allows commitments to be readjusted intraday using updated forecasts could further reduce wind-uncertainty costs [11]. While such measures can affect the specific wind-uncertainty cost and emissions estimates presented here, we expect that our general findings hold, since RTP has tremendous wind-integration benefits regardless of how the stochastic planning model is implemented [30]. Our analysis neglects the effect of transmission constraints. Including such constraints could result in greater wind curtailment [31], [32], which RTP could alleviate [12]. This may yield greater emissions benefits from the combination of wind and RTP, since RTP shifts loads in transmission-constrained regions to periods with excess wind that must otherwise be curtailed. What wind curtailment we observe is due to generator operating constraints, which have a limited impact at the modest wind penetration modeled. At higher penetrations these constraints can limit the amount of wind that the system can accept, which RTP can help mitigate.

An important assumption in evaluating the emissions impacts of RTP without wind is that there are no binding CO_2, SO_2, or NO_x emissions constraints. In the short-run, a binding SO_2 constraint would require operational measures, such as emissions dispatch or fuel switching [33]–[36], which would prevent the change in the fuel mix toward coal. Since we do not consider such a constraint, the emissions estimates for the case with RTP and no wind are illustrative of the effects of RTP if no such restrictions are in place. Our analysis also neglects the locational impacts of generator emissions, which can be important. The effect of NO_x, especially in ozone formation, is highly sensitive to location, temperature, sunlight, and other factors. NO_x can also be transported over regional scales, with associated effects sensitive to dilution, chemical transformation, and deposition during long-range

TABLE VII
TOTAL ANNUAL EMISSIONS OF CO$_2$, SO$_2$, AND NO$_x$ AVERTED BY WIND, PER DOLLAR OF WIND-UNCERTAINTY COST INCURRED

Wind Forecast Error Variance	Fixed Loads			RTP		
	CO$_2$ [t/\$]	SO$_2$ [kg/\$]	NO$_x$ [kg/\$]	CO$_2$ [t/\$]	SO$_2$ [kg/\$]	NO$_x$ [kg/\$]
0.0025	3	6	0	23–232	35–216	1–10
0.0100	2	3	0	6–228	9–215	0–11
0.0225	1	2	0	3–125	5–119	0–6

transport [37]. Our emissions findings are also sensitive to the cost of natural gas, relative to coal, which was quite high in 2005. The recent development of shale gas in North America has significantly reduced this cost difference, and in some cases made natural gas a less costly generation fuel. If such 'cost reversals' are persistent, then the emissions impacts of wind and RTP could be significantly different from our estimates. This is because natural gas-fired generation would be marginal overnight whereas coal-fired generation would be increasingly used during on-peak hours only. Thus, the change in the diurnal load pattern brought on by RTP would not yield the same emissions increases that we estimate. As such, the net effect of RTP and wind together would be similar wind-uncertainty cost savings but greater emissions benefits.

ACKNOWLEDGMENT

REFERENCES

[1] E. A. DeMeo, W. Grant, M. R. Milligan, and M. J. Schuerger, "Wind plant integration," *IEEE Power and Energy Magazine*, vol. 3, pp. 38–46, November-December 2005.

[2] J. C. Smith, M. R. Milligan, E. A. DeMeo, and B. Parsons, "Utility wind integration and operating impact state of the art," *IEEE Transactions on Power Systems*, vol. 22, pp. 900–908, August 2007.

[3] E. A. DeMeo, G. A. Jordan, C. Kalich, J. King, M. R. Milligan, C. Murley, B. Oakleaf, and M. J. Schuerger, "Accommodating wind's natural behavior," *IEEE Power and Energy Magazine*, vol. 5, pp. 59–67, November-December 2007.

[4] A. Papavasiliou and S. S. Oren, "Coupling wind generators with deferrable loads," in *Energy 2030 Conference*. Atlanta, GA, USA: Institute of Electrical and Electronics Engineers, 17-18 November 2008.

[5] M. Klobasa, "Analysis of demand response and wind integration in Germany's electricity market," *IET Renewable Power Generation*, vol. 4, pp. 55–63, January 2010.

[6] R. Sioshansi, "Evaluating the impacts of real-time pricing on the cost and value of wind generation," *IEEE Transactions on Power Systems*, vol. 25, pp. 741–748, April 2010.

[7] K. Dietrich, J. M. Latorre, L. Olmos, and A. Ramos, "Demand response in an isolated system with high wind integration," *IEEE Transactions on Power Systems*, vol. 27, pp. 20–29, February 2012.

[8] W. Katzenstein and J. Apt, "Air emissions due to wind and solar power," *Environmental Science and Technology*, vol. 43, pp. 253–258, January 2009.

[9] F. Bouffard and F. D. Galiana, "Stochastic security for operations planning with significant wind power generation," *IEEE Transactions on Power Systems*, vol. 23, pp. 306–316, May 2008.

[10] J. García-González, R. M. R. de la Muela, L. M. Santos, and A. M. González, "Stochastic joint optimization of wind generation and pumped-storage units in an electricity market," *IEEE Transactions on Power Systems*, vol. 23, pp. 460–468, May 2008.

[11] A. Tuohy, P. Meibom, E. Denny, and M. O'Malley, "Unit commitment for systems with significant wind penetration," *IEEE Transactions on Power Systems*, vol. 24, pp. 592–601, May 2009.

[12] R. Sioshansi and W. Short, "Evaluating the impacts of real-time pricing on the usage of wind generation," *IEEE Transactions on Power Systems*, vol. 24, pp. 516–524, May 2009.

[13] P. A. Ruiz, C. R. Philbrick, E. Zak, K. W. Cheung, and P. W. Sauer, "Uncertainty management in the unit commitment problem," *IEEE Transactions on Power Systems*, vol. 24, pp. 642–651, May 2009.

[14] A. Papavasiliou, S. S. Oren, and R. P. O'Neill, "Reserve requirements for wind power integration: A scenario-based stochastic programming framework," *IEEE Transactions on Power Systems*, vol. 26, pp. 2197–2206, November 2011.

[15] R. P. O'Neill, P. M. Sotkiewicz, B. F. Hobbs, M. H. Rothkopf, and W. R. Stewart, "Efficient market-clearing prices in markets with nonconvexities," *European Journal of Operational Research*, vol. 164, pp. 269–285, 1 July 2005.

[16] S. Borenstein, J. B. Bushnell, and C. R. Knittel, "A Cournot-Nash equilibrium analysis of the New Jersey electricity market," New Jersey Board of Public Utilities, Appendix A of Review of General Public Utilities Restructuring Petition, Final Report, 1997, docket Number EA97060396.

[17] S. Borenstein and S. P. Holland, "On the efficiency of competitive electricity markets with time-invariant retail prices," *The RAND Journal of Economics*, vol. 36, pp. 469–493, Autumn 2005.

[18] C. S. King and S. Chatterjee, "Predicting California demand response," *Public Utilities Fortnightly*, pp. 27–32, July 2003.

[19] C. Loutan and D. Hawkins, "Integration of renewable resources," California Independent System Operator, Tech. Rep., November 2007.

[20] J. Dupačová, N. Gröwe-Kuska, and W. Römisch, "Scenario reduction in stochastic programming," *Mathematical Programming*, vol. 95, pp. 493–511, March 2003.

[21] "The emissions & generation resource integrated database for 2006 (egrid2006) technical support document," Washington, DC, April 2007, prepared for the U.S. Environmental Protection Agency, Acid Rain Division.

[22] E. A. Nadaraya, "On estimating regression," *Theory of Probability and Its Applications*, vol. 9, pp. 141–142, 1964.

[23] G. S. Watson, "Smooth regression analysis," *Sankhya—The Indian Journal of Statistics, Series A*, vol. 26, pp. 359–372, 1964.

[24] R. Sioshansi and P. Denholm, "Emissions impacts and benefits of plug-in hybrid electric vehicles and vehicle to grid services," *Environmental Science and Technology*, vol. 43, pp. 1199–1204, February 2009.

[25] A. Mills, R. Wiser, M. Milligan, and M. O'Malley, "Comment on "air emissions due to wind and solar power"," *Environmental Science and Technology*, vol. 43, pp. 6106–6107, August 2009.

[26] S. T. Lee and Z. A. Yamayee, "Load-following and spinning-reserve penalties for intermittent generation," *IEEE Transactions on Power Apparatus and Systems*, vol. PAS-100, pp. 1203–1211, March 1981.

[27] L. Söder, "Reserve margin planning in a wind-hydro-thermal power system," *IEEE Transactions on Power Systems*, vol. 8, pp. 564–571, May 1993.

[28] R. Doherty and M. O'Malley, "A new approach to quantify reserve demand in systems with significant installed wind capacity," *IEEE Transactions on Power Systems*, vol. 20, pp. 587–595, May 2005.

[29] S. P. Holland and E. T. Mansur, "Is real-time pricing green? the environmental impacts of electricity demand variance," *The Review of Economics and Statistics*, vol. 90, pp. 550–561, November 2008.

[30] S. H. Madaeni and R. Sioshansi, "The impacts of stochastic programming and demand response on wind integration," *Energy Systems*, 2012, forthcoming.

[31] *Study of Electric Transmission in Conjunction with Energy Storage Technology*, Lower Colorado River Authority, Austin, Texas, August 2003, prepared for Texas State Energy Conservation Office.

[32] P. Denholm and R. M. Margolis, "Evaluating the limit of solar photovoltaics (PV) in traditional electric power systems," *Energy Policy*, vol. 35, pp. 2852–2861, 2007.

[33] J. S. Heslin and B. F. Hobbs, "A multiobjective production costing model for analyzing emissions dispatching and fuel switching [of power stations]," *IEEE Transactions on Power Systems*, vol. 4, pp. 836–842, August 1989.

[34] J. H. Talaq, F. El-Hawary, and M. E. El-Hawary, "A summary of environmental/economic dispatch algorithms," *IEEE Transactions on Power Systems*, vol. 9, pp. 1508–1516, August 1994.

[35] E. D. Delarue and W. D. D'haeseleer, "Greenhouse gas emission reduction by means of fuel switching in electricity generation: Addressing the potentials," *Energy Conversion and Management*, vol. 49, pp. 843–853, April 2008.

[36] E. D. Delarue, K. Voorspools, and W. D. D'haeseleer, "Fuel switching in the electricity sector under the EU ETS: Review and prospective," *Journal of Energy Engineering*, vol. 134, pp. 40–46, June 2008.

[37] J. M. Seinfeld and S. N. Pandis, *Atmospheric Chemistry and Physics: From Air Pollution to Climate Change*, 2nd ed. Hoboken, New Jersey, USA: Wiley-Interscience, August 2006.

Seyed Hossein Madaeni (S'11) holds the B.S. and M.S. degrees in electrical engineering from the University of Tehran and the Ph.D. in industrial and systems engineering from The Ohio State University.

He is a Senior Energy Supply Analyst in the Short Term Electric Supply Department at Pacific Gas and Electric Company, San Francisco, CA. His research focuses on electricity market design and mechanisms, renewable energy analysis, and power system operations.

Ramteen Sioshansi (M'11–SM'12) holds the B.A. degree in economics and applied mathematics and the M.S. and Ph.D. degrees in industrial engineering and operations research from the University of California, Berkeley, and an M.Sc. in econometrics and mathematical economics from The London School of Economics and Political Science.

He is an assistant professor in the Integrated Systems Engineering Department at The Ohio State University, Columbus, OH. His research focuses on renewable and sustainable energy system analysis and the design of restructured competitive electricity markets.